

## ***In Situ* Detection of PHIP at 48 mT: Demonstration Using a Centrally Controlled Polarizer**

Kevin W. Waddell, Aaron M. Coffey, and Eduard Y. Chekmenev\*

Vanderbilt University Institute of Imaging Science, 1161 21st Avenue South,  
Nashville, Tennessee 37232, United States

Received September 21, 2010; E-mail: eduard.chekmenev@vanderbilt.edu

**Abstract:** Presented here is a centrally controlled, automated parahydrogen-based polarizer with *in situ* detection capability. A 20% polarization, corresponding to a 5 000 000-fold signal enhancement at 48 mT, is demonstrated on 2-hydroxyethyl-1-<sup>13</sup>C-propionate-*d*<sub>2,3,3</sub> using a double-tuned antenna and pulsed polarization transfer. *In situ* detection is a refinement of first-generation devices enabling fast calibration of rf pulses and *B*<sub>0</sub>, quality assurance of hyperpolarized contrast agents, and stand-alone operation without the necessity of high-field MR spectrometers. These features are essential for biomedical applications of parahydrogen-based hyperpolarization and for clinical translation. We demonstrate the flexibility of the device by recording <sup>13</sup>C signal decay due to longitudinal relaxation of a hyperpolarized contrast agent at 48 mT corresponding to 2 MHz proton frequency. This appears to be the longest recorded *T*<sub>1</sub> (101 ± 7 s) for a <sup>13</sup>C hyperpolarized contrast agent in water.

### Introduction

Nuclear magnetic resonance (NMR) is a relatively insensitive method for detecting metabolites *in vivo* due to low nuclear spin polarization and broad resonances that arise from susceptibility gradients across heterogeneous tissues. Methods for increasing polarization toward the theoretical limit of unity are becoming more widespread and can potentially decrease the metabolite MR detection threshold at available clinical fields from 1 μmol/cm<sup>3</sup> to sub-nmol/cm<sup>3</sup>. For example, the spin polarization available at 3 T and *in vivo* temperatures is *P* = 2.6 × 10<sup>-4</sup> % for <sup>13</sup>C versus *P* = 20% for hyperpolarized samples. These hyperpolarized spin states relax to the equilibrium according to an exponential decay constant *T*<sub>1</sub>. Despite this shortcoming, useful contrast agents with *T*<sub>1</sub> relaxation times on the order of 10–120 s have enabled pathway-specific flux measurements with hyperpolarized samples at unprecedented temporal and spatial resolution *in vivo*.<sup>1</sup> As a result, subsecond metabolic imaging of hyperpolarized agents<sup>1</sup> has the potential to be a sensitive and specific tool for imaging abnormal metabolism such as that of many cancers.<sup>2,3</sup> Not surprisingly, the ongoing research efforts of many groups have been focused on human cancer imaging in preclinical models with Investigational New Drug (IND) and U.S. Food and Drug Administration (FDA) clearance approved<sup>4</sup> for the first clinical trial using

hyperpolarized <sup>13</sup>C-pyruvate (University of California San Francisco).<sup>5</sup> When these methods are refined and improved so as to afford safe administration, hyperpolarized MR is likely to become a pivotal complement to fluorodeoxyglucose-positron emission tomography (FDG-PET) for cancer imaging.<sup>6</sup>

The two dominant technologies for hyperpolarization of exogenous contrast agents are referred to as dynamic nuclear polarization (DNP)<sup>7</sup> and para-hydrogen-induced polarization (PHIP).<sup>8</sup> The latter utilizes facile production of pure singlet states of diatomic hydrogen, whereas the former relies upon polarization transfer from highly polarized electrons in glasses at high magnetic fields and cryogenic temperatures. Despite significant technological challenges and relatively high cost, the DNP technique has progressed to commercially available systems capable of producing batches of hyperpolarized solution every 1–3 h. During this time, polarization buildup is monitored by a high-resolution NMR probe, allowing for optimization of hyperpolarized conditions and quality assurance (QA).

Compared to long preparation periods associated with DNP in current commercial implementations, PHIP can be used to prepare hyperpolarized metabolic contrast agents such as <sup>13</sup>C-succinate in aqueous media in seconds.<sup>9,10</sup> First-generation PHIP polarizer prototypes<sup>10,11</sup> are currently in use by a few scientific

- (1) Golman, K.; in't Zandt, R.; Thaning, M. *Proc. Natl. Acad. Sci. U. S. A.* **2006**, *103*, 11270–11275.
- (2) Day, S. E.; Kettunen, M. I.; Gallagher, F. A.; Hu, D. E.; Lerche, M.; Wolber, J.; Golman, K.; Ardenkjaer-Larsen, J. H.; Brindle, K. M. *Nat. Med.* **2007**, *13*, 1382–1387.
- (3) Gallagher, F. A.; Kettunen, M. I.; Day, S. E.; Hu, D. E.; Ardenkjaer-Larsen, J. H.; in't Zandt, R.; Jensen, P. R.; Karlsson, M.; Golman, K.; Lerche, M. H.; Brindle, K. M. *Nature* **2008**, *453*, 940–U73.
- (4) Kurhanewicz, J.; Vigneron, D.; Brindle, K.; Chekmenev, E.; Comment, A.; Cunningham, C.; DeBerardinis, R.; Green, G.; Leach, M.; Rajan, S.; Rizi, R.; Ross, B.; Warren, W. S.; Malloy, C. *Neoplasia* 2011, accepted for publication.

- (5) Kurhanewicz, J.; Bok, R.; Nelson, S. J.; Vigneron, D. B. *J. Nucl. Med.* **2008**, *49*, 341–344.
- (6) Gambhir, S. S. *Nat. Rev. Cancer* **2002**, *2*, 683–693.
- (7) Abragam, A.; Goldman, M. *Rep. Prog. Phys.* **1978**, *41*, 395–467.
- (8) Bowers, C. R.; Weitekamp, D. P. *J. Am. Chem. Soc.* **1987**, *109*, 5541–5542.
- (9) Chekmenev, E. Y.; Hovener, J.; Norton, V. A.; Harris, K.; Batchelder, L. S.; Bhattacharya, P.; Ross, B. D.; Weitekamp, D. P. *J. Am. Chem. Soc.* **2008**, *130*, 4212–4213.
- (10) Hövener, J.-B.; Chekmenev, E.; Harris, K.; Perman, W.; Robertson, L.; Ross, B.; Bhattacharya, P. *Magn. Reson. Mater. Phys. Biol. Med.* **2009**, *22*, 111–121.
- (11) Goldman, M.; Johannesson, H.; Axelsson, O.; Karlsson, M. *Magn. Reson. Imaging* **2005**, *23*, 153–157.

groups and typically require tedious calibrations. Earlier designs covered the essential experimental demands for proof of concept, but refinements to ease operator demands and to improve robustness will facilitate extension of PHIP as a routine preclinical tool for studying *in vivo* metabolism. A typical PHIP workflow requires calibration of the electromagnet field<sup>10</sup> where catalytic hydrogenation takes place and tedious optimization of applied radiofrequency fields (rf) to accomplish efficient transfer in sequences with 10 or more pulses.<sup>12</sup> Lacking onboard receivers and comprehensive central control, first-generation PHIP devices often require time-consuming calibrations using detection on external high-field spectrometers.<sup>13</sup> These drawbacks limit PHIP technology to a few sites with skilled MR spectroscopists and inhibit a widespread use of this technology for multidisciplinary imaging communities, especially among the biologists, biochemists, and medical researchers.

The instrument presented here addresses additional considerations required for high-throughput *in vivo* studies and is based on an earlier prototype, which operates at a static field of 12 mT (Waddell, K. W., unpublished results). The design is streamlined from commercially available controllers, and the added functionality reduces experimental demands and improves reliability. We provide the overall polarizer design and the basic steps necessary for quick fine-tuning. Sensitivity at 48 mT is sufficient for QA of hyperpolarized contrast agents. The polarizer operates as a stand-alone device to produce hyperpolarized contrast agents for biomedical imaging. Other research groups can readily replicate this polarizer design, because it is based on commercially available low-field NMR equipment. To demonstrate the utility of *in situ* detection and the overall instrument setup, we have measured the lifetime of the hyperpolarized contrast agent, 2-hydroxyethyl-1-<sup>13</sup>C-propionate-*d*<sub>2,3,3</sub> (HEP), at 48 mT, and the resulting *T*<sub>1</sub> appears to be the longest recorded *T*<sub>1</sub> for a <sup>13</sup>C hyperpolarized contrast agent in protonated aqueous medium.

## Methods

**Parahydrogen (para-H<sub>2</sub>) Gas.** para-H<sub>2</sub> (97.5 ± 0.5%) was prepared by passage of high-purity hydrogen gas through a 14 K chamber<sup>14</sup> filled with iron oxide catalyst<sup>10</sup> using an in-house automated para-H<sub>2</sub> generator setup. The fresh para-H<sub>2</sub> obtained over the course of an hour's production was collected in a 10 L aluminum storage tank (200 psi or 14 bar). Percentage of para-H<sub>2</sub> conversion was measured by <sup>1</sup>H spectroscopy using a Bruker 500 MHz high-resolution NMR spectrometer.<sup>15</sup>

**RF Circuit.** A double-tuned rf circuit operating at 2.020 MHz (<sup>1</sup>H) and 0.508 MHz (<sup>13</sup>C) was designed on the basis of a previously published high-field rf circuit.<sup>16</sup> The circuit consists of two coils with elements for achieving suitable tuning range and impedance matching for each channel. The air core inductors were wound from 20 AWG magnet wire. Inductances were *L*<sub>S</sub> = 39.6 μH for the sample coil and *L*<sub>G</sub> = 30.8 μH for the ground coil with impedance matching on the <sup>1</sup>H channel achieved via *L*<sub>MH</sub> = 617 nH as measured on an Agilent E5071C network analyzer. A combination of fixed C22CF series capacitors (Dielectric Laboratories, Cazenovia, NY) were used in parallel with variable capacitors (model

NMTM120C, Voltronics, Denville, NJ). The optimal value of <sup>1</sup>H tuning capacitance was *C*<sub>T1H</sub> = 391 pF + 0–120 pF. For <sup>13</sup>C, the optimal tune and match capacitances were *C*<sub>T13C</sub> = 1100 pF + 0–120 pF and *C*<sub>M13C</sub> = 270 pF + 0–120 pF. Because the measured isolation between channels was –5 dB, an in-line parallel LC circuit serving as a low pass filter for the <sup>1</sup>H frequency was added to the <sup>13</sup>C channel to improve the isolation between the channels.

**Molecular Addition of para-H<sub>2</sub> Using Rh-Based Catalyst.** The molecular addition of para-H<sub>2</sub> gas to the tracer was conducted in the previously described chemical reactor at a 120 psi (8 bar) para-H<sub>2</sub> pressure over a time span of 4 s under the conditions of continuous wave (CW) proton decoupling. The hydrogenation reaction was more than 95% complete using the Rh-based molecular catalyst.<sup>17,18</sup> The catalyst in aqueous medium was prepared using a previously developed protocol<sup>13</sup> to a final catalyst concentration of 2.5–3.0 mM. The molecular precursor, 2-hydroxyethyl-1-<sup>13</sup>C-acrylate-*d*<sub>2,3,3</sub> (HEA; product number 676071, Sigma-Aldrich-Isotec, Miamisburg, OH), was added to freshly prepared catalyst solution resulting in 8 mM HEA. The prepared stock solution containing catalyst and HEA was used for chemical reaction with 97.5% para-H<sub>2</sub>. The reactor pressure after spraying the liquid using high-pressure N<sub>2</sub> gas into an atmosphere of para-H<sub>2</sub> gas was 250 psi or 17 bar.

**Polarization Transfer from para-H<sub>2</sub>.** Spin order of para-H<sub>2</sub> singlet state was converted to <sup>13</sup>C hyperpolarization using the polarization transfer sequence developed by M. Goldman et al.<sup>12</sup> The rf pulses were optimized using the method described in the Results section. Filling the reactor chamber with para-H<sub>2</sub> gas, injecting an aqueous mixture of molecular precursor and catalyst, chemical reaction under CW <sup>1</sup>H decoupling, and heteronuclear polarization transfer were timed from the central controller (Magritek, Wellington, New Zealand). *In situ* NMR detection of hyperpolarized compounds was started immediately after polarization transfer from para-H<sub>2</sub> to <sup>13</sup>C. These contrast agents are expected to be used in high-field *in vivo* imaging, and the automated ejection along with filtration can be seamlessly integrated and systematically controlled with respect to all other experimental events with this setup. Although the catalytic hydrogenation is typically conducted at elevated temperature (>60 °C),<sup>9,15</sup> the ejected material decreases the temperature to 30–35 °C due to sample manipulation, which is compatible with *in vivo* use.

## Results

A commercially available double-channel MR spectrometer (Magritek, Wellington, New Zealand) synchronizes rf transmission, chemical shuttling, and detection in the 48 mT field of a Halbach array. TTL lines are accessed within the pulse program itself and routed through a microcontroller to switch solenoid valves that control gas and chemical delivery to the high-pressure reactor (Figure 1).

**rf and B<sub>0</sub> Calibration.** The frequency response of the <sup>1</sup>H and <sup>13</sup>C channels of a dual-channel probe (described in Methods) is presented in Figure 2. The circuit design achieved a quality factor *Q* = 66 for the <sup>1</sup>H channel at 2.02 MHz and *Q* = 43 for the <sup>13</sup>C channel operated at 0.508 MHz. Radio frequency calibration using a solution of 29 g of sodium 1-<sup>13</sup>C-acetate in 99.9% D<sub>2</sub>O in a 100 mL spherical phantom yielded a 90° <sup>1</sup>H excitation pulse width of 37 μs at 57 W. The corresponding pulse width on <sup>13</sup>C was 150 μs at 14 W. <sup>1</sup>H rf calibration was conducted using an automated routine supplied by the manufacturer of the low-field spectrometer. The calibration of resonant frequencies is conducted by direct proton detection and can be shifted up to ~1 kHz in extreme cases due to spatially heterogeneous spurious magnetic fields that arise from super-

- (12) Goldman, M.; Johannesson, H. C. *R. Phys.* **2005**, *6*, 575–581.
- (13) Hövener, J.-B.; Chekmenev, E.; Harris, K.; Perman, W.; Tran, T.; Ross, B.; Bhattacharya, P. *Magn. Reson. Mater. Phys. Biol. Med.* **2009**, *22*, 123–134.
- (14) Tam, S.; Fajardo, M. E. *Rev. Sci. Instrum.* **1999**, *70*, 1926–1932.
- (15) Bhattacharya, P.; Harris, K.; Lin, A. P.; Mansson, M.; Norton, V. A.; Perman, W. H.; Weitekamp, D. P.; Ross, B. D. *Magn. Reson. Mater. Phys. Biol. Med.* **2005**, *18*, 245–256.
- (16) Zhang, Q. W.; Zhang, H.; Lakshmi, K. V.; Lee, D. K.; Bradley, C. H.; Wittebort, R. J. *J. Magn. Reson.* **1998**, *132*, 167–171.

- (17) Gridnev, I. D.; Higashi, N.; Asakura, K.; Imamoto, T. *J. Am. Chem. Soc.* **2000**, *122*, 7183–7194.
- (18) Gridnev, I. D.; Imamoto, T. *Acc. Chem. Res.* **2004**, *37*, 633–644.

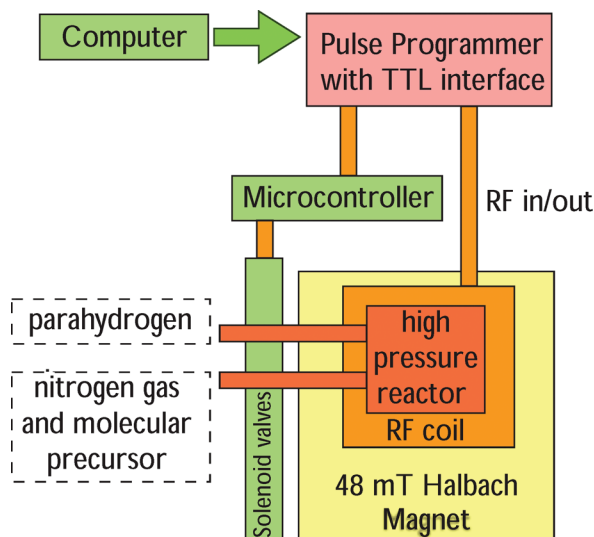


Figure 1. PHIP polarizer schematic.

position of interfering fields and potential coupling of  $B_0$  to nearby objects. Additional resonant frequencies ( $^{13}\text{C}$ ,  $^{15}\text{N}$ ,  $^{23}\text{Na}$ , etc.) scale according to gyromagnetic ratios and are calculated based on the proton Larmor frequency.

**Reactor.** The details of molecular addition of parahydrogen ( $\text{para-H}_2$ ) and polarization transfer from  $\text{para-H}_2$  protons to X nuclei are described in Methods. The reactor allows spraying of the aqueous mixture of unsaturated molecular precursor and the catalyst into pressurized  $\text{para-H}_2$  gas (120 psi or 8 bar). Reaction surface area is maximized by pushing the solution through a cluster of  $<0.25$  mm holes with nitrogen gas (250 psi or 17 bar) into a 2 in. (o.d.) cylindrical polysulfone reactor that can withstand 280 psi (19 bar) and  $60^\circ\text{C}$ . The key requirement for efficient performance of the polarization transfer sequence<sup>12</sup> of PHIP hyperpolarization, as depicted in Figure 3, is good rf homogeneity of the sample coil ( $L_S$ ) over the entire reactor volume.  $B_1$  homogeneity was tested by measuring the signal magnitude between  $450^\circ$  and  $90^\circ$  pulses, with a sample of 60 mL of  $\text{H}_2\text{O}$  and doped with 5 mM  $\text{CuSO}_4$ . The homogeneity of the  $^1\text{H}$  channel measured in this way was 96% and dropped off modestly to 90% when comparing the signal at  $810^\circ$  and  $90^\circ$  pulses.

**In Situ Quality Assurance of PHIP Hyperpolarization.** The *in situ* measurement of percentage (%) hyperpolarization is demonstrated in Figure 4b. To maximize signal-to-noise ratio (SNR), the  $^{13}\text{C}$  spectrum of hyperpolarized HEP was acquired with  $90^\circ$  excitation pulses. The reference  $^{13}\text{C}$  spectrum of sodium 1- $^{13}\text{C}$ -acetate solution in  $\text{D}_2\text{O}$  ( $^{13}\text{C}$   $T_1 = 18 \text{ s} \pm 2 \text{ s}$  at 48 mT, data not shown), Figure 4a, was used to calculate % hyperpolarization ( $\%P_{\text{HP}}$ ). We have used thermal  $^{13}\text{C}$  polarization ( $\%P_{\text{TP}}$  =  $4 \times 10^{-6}$  % at 48 mT and 298 K) of 29 g of sodium 1- $^{13}\text{C}$ -acetate to calculate % hyperpolarization as follows:

$$\%P_{\text{HP}} = \%P_{\text{TP}} \frac{n_{\text{TP}}}{n_{\text{HP}}} \frac{S_{\text{HP}}}{S_{\text{TP}}} = \%P_{\text{TP}} \epsilon$$

with

$$\epsilon = \frac{n_{\text{TP}}}{n_{\text{HP}}} \frac{S_{\text{HP}}}{S_{\text{TP}}}$$

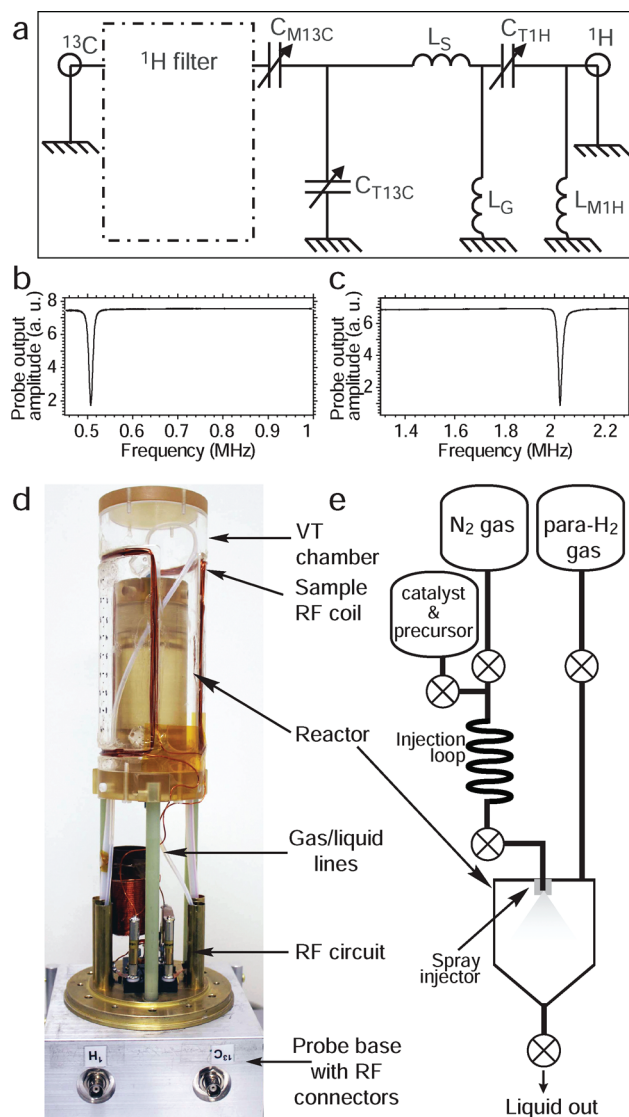


Figure 2. NMR probe design. (a) Diagram of the double resonance rf circuit tuned to 2.02 and 0.508 MHz, respectively, for  $^1\text{H}$  and  $^{13}\text{C}$  (at 48 mT), (b) frequency sweep response of  $^{13}\text{C}$  channel resonating at 0.508 MHz, (c) frequency sweep response of  $^1\text{H}$  channel resonating at 2.02 MHz, (d) photograph of rf probe showing sample coil wrapped around a 60 mL reactor chamber that is positioned in the magnet isocenter, (e) the diagram of polarizer components operated with solenoids  $\otimes$ .

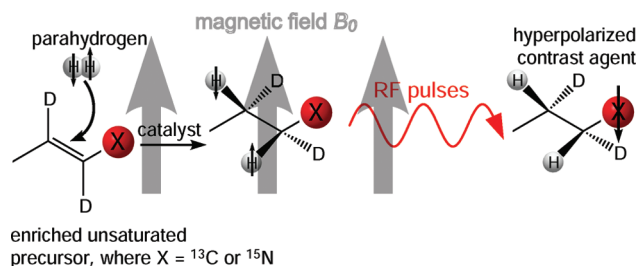
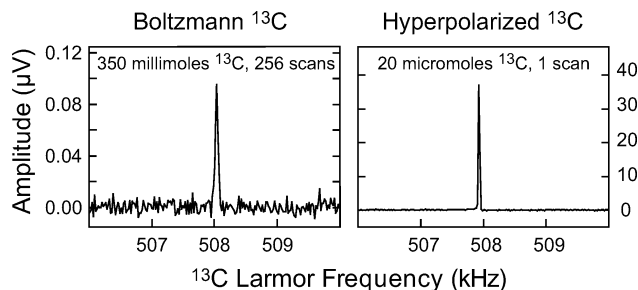


Figure 3. Schematic of spin-order transfer from singlet states of  $\text{para-H}_2$  spins to X nuclei, where X is  $^{13}\text{C}$  or  $^{15}\text{N}$ . Unsaturated molecular precursor carrying D and X labels undergoes catalytic molecular *cis*-addition of  $\text{para-H}_2$  in the presence of a magnetic field under  $^1\text{H}$  decoupling followed by rf pulses on  $^1\text{H}$  and X. Radio frequency pulses transfer hyperpolarization from nascent protons to X nuclei.<sup>12</sup> The entire process is automated.

where  $n_{\text{HP}}$  and  $n_{\text{TP}}$  are the molar quantities of hyperpolarized contrast agent and thermally polarized reference samples,





**Figure 4.** *In situ* NMR in PHIP polarizer utilizing 48 mT permanent magnet. (a)  $^{13}\text{C}$  spectrum of 29 g (350 mmol) of 3.5 M sodium 1- $^{13}\text{C}$ -acetate in 100 mL of  $\text{D}_2\text{O}$  acquired with 256 scans and 200 s repetition time; (b) single scan spectrum of  $^{13}\text{C}$  hyperpolarized 8 mM 2-hydroxyethyl-1- $^{13}\text{C}$ -propionate- $d_{2,3,3}$  (HEP), 3 mL containing  $\sim 2 \times 10^{-5}$  mol, using the same acquisition parameters. Polarization  $\%P_{\text{HP}} = 20\%$ ; signal enhancement  $\epsilon \approx 5\,000\,000$  fold.

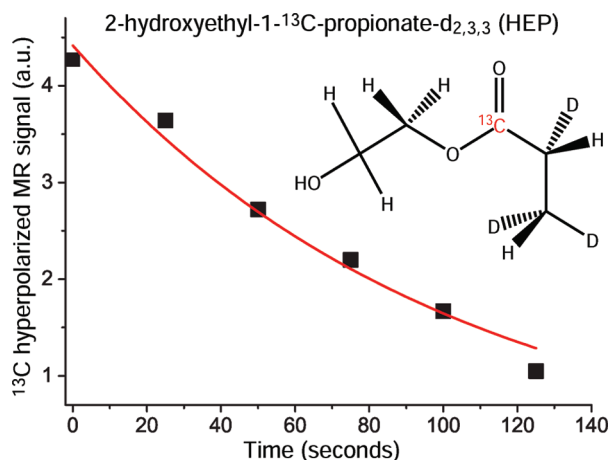


**Figure 5.**  $^{13}\text{C}$   $T_1$  measurement of hyperpolarized 2-hydroxyethyl-1- $^{13}\text{C}$ -propionate- $d_{2,3,3}$  (HEP) in water and  $B_0 = 48$  mT using polarization decay method.  $T_1 = 101 \pm 7$  s,  $R^2 = 0.98$ .  $^{13}\text{C}$  signals were acquired with  $30^\circ$  excitation angle rf pulse. Fitted data (red) account for  $^{13}\text{C}$  polarization loss due to excitation pulses. The size of the squares corresponds to the estimated experimental errors in measured signal and time.

respectively.  $S_{\text{HP}}$  and  $S_{\text{TP}}$  are the corresponding MR signals (acquired using identical parameters).  $\epsilon$  is the signal enhancement ratio. Polarization  $\%P_{\text{HP}} = 20\%$  and  $^{13}\text{C}$  signal enhancement  $\epsilon \approx 5\,000\,000$ -fold were achieved.

**Spin–Lattice Relaxation of Hyperpolarized Contrast Agent at 48 mT.** The *in situ* detection capability of the polarizer was utilized to measure the decay of  $^{13}\text{C}$  hyperpolarized HEP, Figure 5. The decay of hyperpolarization to thermal equilibrium was monitored by  $30^\circ$  excitation rf pulses. Polarization loss of  $\sim 13\%$  due to rf excitation by each pulse was included in the fit of exponential decay ( $T_1 = 101 \pm 7$  s,  $R^2 = 0.98$ ). To the best of our knowledge, this represents the longest  $T_1$  of any  $^{13}\text{C}$  hyperpolarized contrast agent in  $\text{H}_2\text{O}$  (l). In a previous experiment where HEP was used for *in vivo* angiography,<sup>11</sup> the  $^{13}\text{C}$   $T_1$  at 4.7 T was reported to be 50 s *in vitro*.<sup>13</sup> The consequences of such long  $^{13}\text{C}$   $T_1$  are discussed below.

## Discussion

Figure 4 demonstrates that the extent of hyperpolarization can be measured *in situ* in a low 48 mT field in micromolar quantities using oversized detection coils and direct detection using  $^{13}\text{C}$  spectroscopy. The described method provides a convenient approach to QA of PHIP polarization for  $B_1$  and  $B_0$  calibration as well as hyperpolarization extent. These attributes

should facilitate increased throughput and more robust operation for *in vivo* experiments on PHIP metabolic contrast agents. Because the described polarizer design is based on a commercially available, low-field magnet and MR spectrometer, it is accessible to scientists with interests in studying fast metabolism but expertise outside of NMR and at a fraction of the upfront equipment and running costs of competing DNP devices.

While optimization of polarization toward the theoretical limit is outside of the scope of this work, the  $\%P_{\text{HP}}$  reported here (20%) is consistent with levels published<sup>10,11</sup> using earlier designs. On the basis of SNR, Figure 4b, we estimate that the detection QA threshold at 48 mT for this instrument is one micromole of hyperpolarized contrast agent. The level of sensitivity demonstrated here for 20 micromoles of hyperpolarized contrast agent should also enable QA detection at significantly lower  $B_0$  fields, which can also be conveniently generated by an electromagnet. The qualitative comparison of the  $^{13}\text{C}$  hyperpolarized detection sensitivity with that of hyperpolarized  $^{129}\text{Xe}$  low-field polarimetry<sup>19</sup> shows that it is  $\sim 2$  orders of magnitude greater in our polarizing setup. This sensitivity gain is largely attributed to the use of a tunable rf coil, better rf noise isolation, and a higher and more homogeneous  $B_0$  field magnet.

The described implementation of this PHIP polarizer should enable robust operation by nonspecialists and will help to stimulate more research in the area. Higher participation in PHIP research will presumably increase the pipeline of unsaturated precursors, which currently limits the spectrum of applications for para- $\text{H}_2$  based experiments. This model of adoption has certainly been verified in DNP, where the number of precursors is expanding rapidly. A small albeit diverse group of important PHIP precursors are already established and provide a springboard for more development. A partial list of these compounds and targets is (1) tetrafluoropropyl 1- $^{13}\text{C}$ -propionate- $d_{2,3,3}$ <sup>20</sup> for plaque imaging, (2) succinate<sup>9,21,22</sup> for metabolic imaging of cancer, and (3) a glucose analogue<sup>23</sup> that is functionally similar to fluorodeoxyglucose (FDG).

Although we have demonstrated PHIP using the PASADENA effect<sup>8</sup> in a homogeneous aqueous medium, this polarizer design with *in situ* detection capability should be especially useful for studying proposed heterogeneous PHIP catalysts<sup>24</sup> and could also be translated to the signal amplification by the reversible exchange (SABRE)<sup>25</sup> method of hyperpolarization. The latter method produces highly polarized proton sites that are in close proximity to metal hydride exchange sites in a magnetic field of a few mT. Therefore a low-field polarizer would allow for intermolecular polarization transfer from highly polarized

- (19) Nikolaou, P.; Whiting, N.; Eschmann, N. A.; Chaffee, K. E.; Goodson, B. M.; Barlow, M. J. *J. Magn. Reson.* **2009**, *197*, 249–254.
- (20) Chekmenev, E. Y.; Norton, V. A.; Weitekamp, D. P.; Bhattacharya, P. *J. Am. Chem. Soc.* **2009**, *131*, 3164–3165.
- (21) Bhattacharya, P.; Chekmenev, E. Y.; Perman, W. H.; Harris, K. C.; Lin, A. P.; Norton, V. A.; Tan, C. T.; Ross, B. D.; Weitekamp, D. P. *J. Magn. Reson.* **2007**, *186*, 150–155.
- (22) Ross, B. D.; Bhattacharya, P.; Wagner, S.; Tran, T.; Sailasuta, N. *Am. J. Neuroradiol.* **2010**, *31*, 24–33.
- (23) Reineri, F.; Santelia, D.; Viale, A.; Cerutti, E.; Poggi, L.; Tichy, T.; Premkumar, S. S. D.; Gobetto, R.; Aime, S. *J. Am. Chem. Soc.* **2010**, *132*, 7186–7193.
- (24) Kovtunov, K. V.; Beck, I. E.; Bukhtiyarov, V. I.; Koptuyug, I. V. *Angew. Chem., Int. Ed.* **2008**, *47*, 1492–1495.
- (25) Adams, R. W.; Aguilar, J. A.; Atkinson, K. D.; Cowley, M. J.; Elliott, P. I. P.; Duckett, S. B.; Green, G. G. R.; Khazal, I. G.; Lopez-Serrano, J.; Williamson, D. C. *Science* **2009**, *323*, 1708–1711.

SABRE protons to longer-lived  $^{13}\text{C}$  or  $^{15}\text{N}$  sites with the goal of preserving the induced hyperpolarization for biomedical imaging.

As a demonstration of the practical utility of *in situ* detection, the lifetime of hyperpolarized HEP contrast agents was measured. The  $^{13}\text{C}$   $T_1$  (101 s) at 48 mT reported here is double the recently reported high-field value in protonated aqueous medium ( $^{13}\text{C}$   $T_1$  = 50 s at 4.7 T) under otherwise identical conditions.<sup>13</sup> Since the MR sensitivity of hyperpolarized *in vivo* imaging has a weak dependence on the magnetic field strength and peaks at magnetic fields below 0.5 T,<sup>26</sup> low-field imaging of exogenous hyperpolarized contrast agents may have significant advantages

due to much longer lifetimes of hyperpolarized contrast agents similar to the one studied here.

**Acknowledgment.** We wish to thank for funding support ICMIC 5P50 CA128323-03, NIH R00 1R00CA13474 9, R25 CA136440, 3R00CA134749-02S1, and Prevent Cancer Foundation. We thank Dr. Bibo Feng, Ken Wilkens, and Dr. Sasidhar Tadanki for discussions and engineering support.

JA108529M

---

(26) Parra-Robles, J.; Cross, A. R.; Santyr, G. E. *Med. Phys.* **2005**, *32*, 221–229.